Computer simulation of ferroelectric domain structures in epitaxial $BiFeO_3$ thin films

J. X. Zhang,[1,a)] Y. L. Li,[1] S. Choudhury,[1] L. Q. Chen,[1] Y. H. Chu,[2] F. Zavaliche,[2] M. P. Cruz,[2,b)] R. Ramesh,[2] and Q. X. Jia[3]
[1]*Department of Materials Science and Engineering, Pennsylvania State University, University Park, Pennsylvania 16802, USA*
[2]*Department of Materials Science and Engineering and Department of Physics, University of California, Berkeley, California 94720, USA*
[3]*MPA-STC, Los Alamos National Laboratory, Los Alamos, New Mexico 87545, USA*

(Received 13 December 2007; accepted 16 March 2008; published online 13 May 2008)

Ferroelectric domain structures of $(001)_c$, $(101)_c$, and $(111)_c$ oriented epitaxial $BiFeO_3$ thin films were studied by using the phase-field approach. Long-range elastic and electrostatic interactions were taken into account. The effects of various types of substrate constraint on the domain morphologies were systematically analyzed. It is demonstrated that domain structures of $BiFeO_3$ thin films could be controlled by selecting proper film orientations and substrate constraint. The dependence of the $\{110\}_c$-type domain wall orientation on substrate constraint for the $(001)_c$ oriented $BiFeO_3$ thin film was also discussed. © *2008 American Institute of Physics*.
[DOI: 10.1063/1.2927385]

I. INTRODUCTION

$BiFeO_3$ has attracted a great deal of attention recently due to the coexistence of ferroelectricity and antiferromagnetism at room temperature.[1–8] Bulk $BiFeO_3$ single crystals have a Curie temperature of $T_C \approx 1103$ K, and a Néel temperature of $T_N \approx 643$ K. The ferroelectric phase of $BiFeO_3$ has a rhombohedrally distorted perovskite structure with space group $R3c$. The spontaneous polarization of $BiFeO_3$ is along the pseudocubic $\langle 111\rangle_c$, leading to the formation of eight possible polarization variants: $r_1^+=[111]_c$, $r_2^+=[\bar{1}11]_c$, $r_3^+=[\bar{1}\bar{1}1]_c$, $r_4^+=[1\bar{1}1]_c$, $r_1^-=[\bar{1}\bar{1}\bar{1}]_c$, $r_2^-=[1\bar{1}\bar{1}]_c$, $r_3^-=[11\bar{1}]_c$, and $r_4^-=[\bar{1}1\bar{1}]_c$. Experimentally, a number of different domain structures in $BiFeO_3$ films have been observed.[9–12] Recent studies have demonstrated the ability to manipulate the ferroelectric domain structures by using vicinal substrates or controlling the growth mode for the bottom electrode.[13,14] Therefore, the study of the ferroelectric domain structures of variously oriented epitaxial $BiFeO_3$ thin films is expected to provide guidance to modify ferroelectric properties by heteroepitaxy and strain engineering.

In this work, we employ the phase-field approach to investigate the ferroelectric domain structures in epitaxial $BiFeO_3$ thin films. The phase-field simulation is based on the time-dependent Ginzburg–Landau (TDGL) equation, which takes into account the long-range elastic and electrostatic interactions. It has been extensively used to study the ferroelectric domain structures in both bulk systems and thin films.[15–19] The $BiFeO_3$ film considered here is assumed to be a single crystal having a stress-free top surface and subject to substrate constraint. The main focus of this paper is on the ferroelectric domain structures of variously oriented $BiFeO_3$ thin films as a function of substrate constraint. This paper is organized as follows: in Sec. II, a phase-field model to describe ferroelectric domain structure evolution is introduced. Sec. III presents the simulation results on the domain structures of the $(100)_c$, $(101)_c$, and $(111)_c$ oriented $BiFeO_3$ thin films, and conclusions are summarized in Sec. IV.

II. PHASE-FIELD MODEL

To study the domain structures of the $(001)_c$, $(101)_c$, and $(111)_c$ oriented $BiFeO_3$ thin films, we introduce two coordinate systems: (I): $\mathbf{x}$ (x_1,x_2,x_3) with x_1, x_2, x_3 along the $[100]_c$, $[010]_c$, and $[001]_c$ directions of the pseudocubic cell and (II): $\mathbf{x}'$ (x_1',x_2',x_3') with x_3' out of the film surface, and x_1' and x_2' are in plane. For $(001)_c$ films, x_1', x_2', and x_3' are along the $[100]_c$, $[010]_c$, and $[001]_c$ directions, which are coincident with the coordinate system I. For $(101)_c$ films, x_1', x_2', and x_3' are along the $[010]_c$, $[\bar{1}01]_c$, and $[101]_c$ directions, respectively. While for $(111)_c$ films, x_1', x_2', and x_3' are along the $[01\bar{1}]_c$, $[\bar{2}11]_c$, and $[111]_c$ directions. The polarization vector in the coordinate system II, $\mathbf{P}'(P_1',P_2',P_3')$, is chosen to be the order parameter to describe the ferroelectric domain structures.

The total free energy of a $BiFeO_3$ thin film includes the bulk free energy F_{bulk}, domain wall energy F_{wall}, elastic energy F_{elas}, and electrostatic energy F_{elec}, i.e.,

$$F = F_{\text{bulk}} + F_{\text{wall}} + F_{\text{elas}} + F_{\text{elec}}. \tag{1}$$

The bulk free energy density is described by a conventional Landau-type of expansion

$$F_{\text{bulk}} = \int [\alpha_1(P_1^2+P_2^2+P_3^2) + \alpha_{11}(P_1^4+P_2^4+P_3^4) + \alpha_{12}(P_1^2P_2^2+P_1^2P_3^2+P_2^2P_3^2)]dV, \tag{2}$$

where α_1 and α_{ij} are the phenomenological coefficients

[a)]Electronic mail: jzz108@psu.edu.
[b)]On leave from Centro de Ciencias de la Materia Condensada, Universidad Nacional Autónoma de México, Ensenada, B. C. 22800, Mexico.

 © 2008 American Institute of Physics

Downloaded 19 Oct 2008 to 66.71.79.131. Redistribution subject to AIP license or copyright; see http://jap.aip.org/jap/copyright.jsp

which determine the transition temperature, the spontaneous polarization, and the dielectric susceptibility of the bulk crystal. P_j are the polarization components in the coordinate system I, which are related to P_i' through

$$P_i' = t_{ij} P_j, \tag{3}$$

where t_{ij} is the transformation matrix from the coordinate system I to the coordinate system II. The transformation matrix for the $(001)_c$, $(101)_c$, and $(111)_c$ oriented films are given as follows:

$$t_{ij}^{(001)_c} = \begin{pmatrix} 1 & 0 & 0 \\ 0 & 1 & 0 \\ 0 & 0 & 1 \end{pmatrix},$$

$$t_{ij}^{(101)_c} = \begin{pmatrix} 0 & 1 & 0 \\ -\frac{1}{\sqrt{2}} & 0 & \frac{1}{\sqrt{2}} \\ \frac{1}{\sqrt{2}} & 0 & \frac{1}{\sqrt{2}} \end{pmatrix},$$

$$t_{ij}^{(111)_c} = \begin{pmatrix} 0 & \frac{1}{\sqrt{2}} & \frac{-1}{\sqrt{2}} \\ \frac{-2}{\sqrt{6}} & \frac{1}{\sqrt{6}} & \frac{1}{\sqrt{6}} \\ \frac{1}{\sqrt{3}} & \frac{1}{\sqrt{3}} & \frac{1}{\sqrt{3}} \end{pmatrix}. \tag{4}$$

Assuming that polarization varies continuously across domain boundaries, the domain wall energy can be introduced through the gradients of the polarization field. For the sake of simplicity, we assume the domain wall energy to be isotropic, therefore it can be written as

$$F_{\text{wall}} = \int \frac{1}{2} G_{11} [(P_{1,1}')^2 + (P_{1,2}')^2 + (P_{1,3}')^2 + (P_{2,1}')^2 + (P_{2,2}')^2 + (P_{2,3}')^2 + (P_{3,1}')^2 + (P_{3,2}')^2 + (P_{3,3}')^2] dV, \tag{5}$$

where $P_{i,j}' = \partial P_i' / \partial x_j'$ and G_{11} is gradient energy coefficient.

To consider the dipole-dipole interaction during ferroelectric domain evolution, the electrostatic energy of a domain structure is introduced through

$$F_{\text{elec}} = -\frac{1}{2} \int \mathbf{E}' \cdot \mathbf{P}' dV, \tag{6}$$

where the electric field $\mathbf{E}'$ depends on the polarization distribution and the electric boundary conditions on the film surfaces. Calculation of electric fields is presented in Ref. 18.

If we assume that the interfaces developed during the ferroelectric phase transition as well as the interface between the film and the substrate are coherent, elastic strains will be generated in order to accommodate the structural changes, which are given by

$$e_{ij}' = \varepsilon_{ij}' - (\varepsilon_{ij}^0)', \tag{7}$$

where e_{ij}', ε_{ij}', and $(\varepsilon_{ij}^0)'$ are the elastic strains, total strains, and stress-free strains in the coordinate system II, respectively. The stress-free strains due to electrostrictive effect can be obtained from

$$(\varepsilon_{ij}^0)' = t_{im} t_{jn} (Q_{mnop} P_o P_p), \tag{8}$$

where Q_{mnop} are the electrostrictive coefficients of $BiFeO_3$ in the coordinate system I. The corresponding elastic energy can be expressed as

$$F_{\text{elas}} = \frac{1}{2} \int c_{ijkl}' e_{ij}' e_{kl}' dV = \frac{1}{2} \int c_{ijkl}' [\varepsilon_{ij}' - (\varepsilon_{ij}^0)'][\varepsilon_{kl}' - (\varepsilon_{kl}^0)'] dV, \tag{9}$$

where c_{ijkl}' are the elastic stiffness tensor in the coordinate system II. The equilibrium strains satisfy the mechanical equilibrium condition given by $\sigma_{ij,j}' = 0$, where σ_{ij}' are the stress components and are given by $\sigma_{ij}' = c_{ijkl}' e_{kl}'$. The mechanical boundary condition is such that the top film surface is stress-free, i.e., $\sigma_{i3}'^{\text{top film surface}} = 0$ while the film-substrate surface is coherently constrained by the substrate. The calculation of elastic energy for a film-substrate system[17] is obtained by using a combination of Khachaturyan's mesoscopic elasticity theory[20] and the Stroh formalism of anisotropic elasticity.[21]

The temporal evolution of the polarization field $\mathbf{P}'$ is described by the TDGL equations

$$\frac{\partial P_i'(t)}{\partial t} = -L \frac{\delta F}{\delta P_i'(t)}, \tag{10}$$

where L is a kinetic coefficient related to the domain evolution.

III. FERROELECTRIC DOMAIN STRUCTURES OF $(001)_C$, $(101)_C$, AND $(111)_C$ ORIENTED $BiFeO_3$ THIN FILMS

The temporal evolution of the polarization and thus the domain structures are obtained by numerically solving the TDGL equations using the semi-implicit Fourier spectral method.[22] In the computer simulation, we employed a model of $128\Delta \times 128\Delta \times 32\Delta$, with Δ being the grid size, and periodic boundary conditions are applied along the x_1' and x_2' axes in the film plane. The thickness of the film is taken as $h_f = 16\Delta$. The material constants for the Landau free energy and the nonzero electrostrictive coefficients are from the literature:[23] $\alpha_1 = 4.9(T-1103) \times 10^5$ C^{-2} m^2 N, $\alpha_{11} = 5.42 \times 10^8$ C^{-4} m^6 N, $\alpha_{12} = 1.54 \times 10^8$ C^{-4} m^6 N,[24] $Q_{1111} = 0.032$ C^{-2} m^4, $Q_{1122} = -0.016$ C^{-2} m^4, and $Q_{1212} = 0.01$ C^{-2} m^4, where T is temperature in Kelvin. As we focus on the domain structure of $BiFeO_3$ thin films at room temperature, the temperature is chosen to be $T = 300$ K. For the calculation of elastic energy, we take the elastic constants to be isotopic and homogeneous, with shear modulus $\mu = 0.69 \times 10^{11}$ N m^{-2} and Poisson's ratio $\nu = 0.35$, in order to avoid solving inhomogeneous elastic equations. The cell size in real space is chosen to be $\Delta = l_0$, where $l_0 = \sqrt{G_{110}/\alpha_0}$ and

Downloaded 19 Oct 2008 to 66.71.79.131. Redistribution subject to AIP license or copyright; see http://jap.aip.org/jap/copyright.jsp

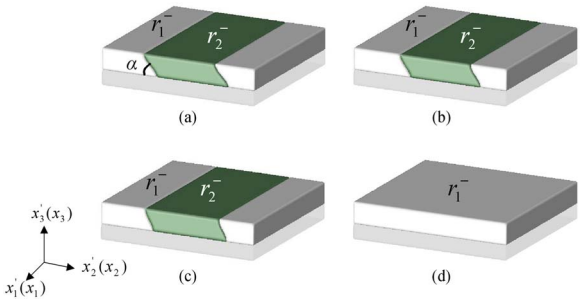

FIG. 1. (Color online) Domain structures of $(001)_c$ $BiFeO_3$ thin films. (a) $\varepsilon_{11}'=\varepsilon_{22}'=-0.01, \varepsilon_{12}'=0$; (b) $\varepsilon_{11}'=\varepsilon_{22}'=0, \varepsilon_{12}'=0$; (c) $\varepsilon_{11}'=\varepsilon_{22}'=0.01, \varepsilon_{12}'=0$; and (d) $\varepsilon_{11}'=\varepsilon_{22}'=0, \varepsilon_{12}'=0.005$.

$\alpha_0=|\alpha_1|_{T=300\ \mathrm{K}}$. We choose the gradient energy coefficient as $G_{11}/G_{110}=0.6$. If $l_0=0.5$ nm, $G_{110}=0.98\times10^{-10}$ $\mathrm{C^{-2}\,m^4\,N}$, and the domain wall energy density is about 0.09 $\mathrm{J\,m^{-2}}$ for 71° domain walls. Short-circuit surface boundary condition is used in the following domain structure simulations, i.e., the electric potentials are equal to zero on both the top film surface and film-substrate interface, which can be achieved by placing top and bottom electrodes when letting both electrodes grounded. The initial polarization is created by assigning a zero value at each grid point plus a small random noise with uniform distribution.

The macroscopic constraint from the substrate depends on the lattice parameters and orientations of the film and substrate. For a $(001)_c$ $BiFeO_3$ thin film epitaxially grown on a $(001)_c$ oriented cubic single crystal substrate with an in-plane orientation relationship of $[100]_c^{\mathrm{BiFeO_3}}\|[100]_c^s$, a constant dilatational plane strain, so-called biaxial strain, is imposed in x_1'-x_2' $(x_1$-$x_2)$ plane,

$$\overline{\varepsilon_{11}'}=\overline{\varepsilon_{22}'}=\varepsilon_0, \quad \overline{\varepsilon_{12}'}=0, \tag{11}$$

where $\varepsilon_0=(a_s-a_{\mathrm{BiFeO_3}})/a_{\mathrm{BiFeO_3}}$, a_s and $a_{\mathrm{BiFeO_3}}$ are the lattice parameters of the substrate and film, respectively. Figure 1 shows the domain structures of $(001)_c$ $BiFeO_3$ thin films from the phase-field simulations, which correspond to different substrate constraints: (a) $\varepsilon_0=-0.01$, (b) $\varepsilon_0=0$, and (c) $\varepsilon_0=0.01$. Similar twinlike domain structures were obtained in all cases with domain walls that separate the rhombohedral variants along the $(011)_c$ planes, which satisfy the elastic compatibility and charge compatibility conditions.[25] We calculated the volume average of the polarization components over the domain structure (the domain wall regions were excluded) for the three different substrate constraints: (a) $\overline{|P_1|}=0.485$, $\overline{|P_2|}=0.487$, $\overline{|P_3|}=0.601$, $\overline{P_s}=0.912$ (b) $\overline{|P_1|}=0.523$, $\overline{|P_2|}=0.526$, $\overline{|P_3|}=0.530$, $\overline{P_s}=0.911$ and (c) $\overline{|P_1|}=0.560$, $\overline{|P_2|}=0.562$, $\overline{|P_3|}=0.447$, $\overline{P_s}=0.910$ ($P_s=|\mathbf{P}|$, unit: $\mathrm{C\,m^{-2}}$). It is seen that $\overline{|P_1|}$ and $\overline{|P_2|}$ are close to each other but different from $\overline{|P_3|}$ because of the substrate constraint. The compressive substrate strain increases $|P_3|$ while tensile strain suppresses it. However, the average spontaneous polarization $\overline{P_s}$ does not change much with the in-plane biaxial substrate strains, which agree well with recent thermodynamic calculations.[23] It should be emphasized that more than one type of twins are available by various combinations of polarization variants, and they are degenerate in energy. Without any external factor that breaks the degeneracy, all types are equally probable to exist, and they could even coexist in a film as it has been observed experimentally.[13]

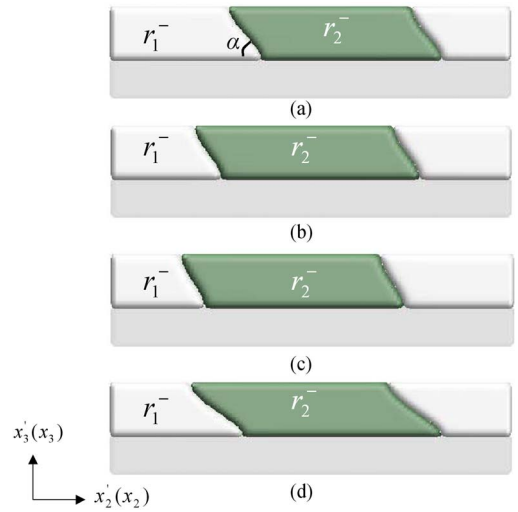

FIG. 2. (Color online) Domain structures of $(001)_c$ $BiFeO_3$ thin films under $\varepsilon_{11}'=\varepsilon_{22}'=-0.005, \varepsilon_{12}'=0$: (a) $G_{11}/G_{110}=0.6$; (b) $G_{11}/G_{110}=0.9$; (c) $G_{11}/G_{110}=1.2$; and (d) $G_{11}/G_{110}=0.6$, $Q_{44}^*=1.5\times Q_{44}$.

Figure 1 also indicates that the $(011)_c$ domain wall deviates from its ideal orientation (for which the angle α between domain wall and the film/substrate interface is equal to 45°). Following the approach of Streiffer *et al.*,[25] the domain wall plane satisfying the elastic compatibility conditions can be determined. For example, considering the domain wall plane between variants r_1^- and r_2^-, the calculated domain wall planes are $(100)_c$ and $(0\ h\ 1)_c$, where $h=|P_2/P_3|$. It is noted that Streiffer *et al.* assumed that $|P_2|=|P_3|$ in their original approach, therefore, the corresponding domain wall planes obtained are $(100)_c$ and $(011)_c$. However, as we discussed above, for a compressive substrate strain, $|P_2|<|P_3|$. Therefore, a compressive substrate strain decreases $\alpha=\arctan(h)$ whereas a tensile substrate strain increases it, as $|P_2|>|P_3|$ under a tensile substrate strain, which is consistent with our phase-field simulation results, as shown in Figs. 1(a)–1(c). However, the angle α obtained is larger than 45° even for a compressive substrate strain [as shown in Fig. 2(a)], which cannot be explained using elastic energy consideration only. Another energy contribution that could affect the domain wall orientation is the total domain wall energy of a domain structure, which prefers the domain walls perpendicular to the film/substrate interface ($\alpha=90°$) to minimize the total domain wall area. It should be noted that the electrostatic energy has no effect on the angle α, since the charge compatibility condition is fulfilled for any domain walls that parallel to the $[100]_c$ direction. In order to understand the role of the total domain wall energy on the domain wall orientation, we performed simulations with artificially increased gradient coefficient G_{11}/G_{110}. Figures 2(b) and 2(c) display the domain structures obtained by fixing $G_{11}/G_{110}=0.9$ and 1.2, respectively. One can see that α increases with the increasing of gradient coefficient. As a comparison, we also conducted a simulation with increased electrostrictive coefficient $Q_{44}^*=1.5Q_{44}$ ($G_{11}/G_{110}=0.6$). A very small α was obtained, as shown in Fig. 2(d), since the elastic energy dominates in this

Downloaded 19 Oct 2008 to 66.71.79.131. Redistribution subject to AIP license or copyright; see http://jap.aip.org/jap/copyright.jsp

case and compressive substrate strains prefer a smaller α as we discussed above. From these simulations, we may conclude that the equilibrium orientations of the $\{110\}_c$ type domain walls are determined by the competition between total domain wall energy and elastic energy.

Shear substrate strain may also exist for $(001)_c$ oriented $BiFeO_3$ thin films, i.e., $\overline{\varepsilon'_{11}}=\overline{\varepsilon'_{22}}\neq 0$, $\overline{\varepsilon'_{12}}\neq 0$. An example is a $(001)_c$ oriented $BiFeO_3$ thin film constrained by a $(001)_o$ orthorhombic substrate with in-plane orientation relationships of $[100]_c^{BiFeO_3}\|[1\bar{1}0]_o^s$ and $[010]_c^{BiFeO_3}\|[\bar{1}10]_o^s$. The shear substrate strain $\varepsilon'_{12}=\gamma-\pi/2$, where γ is the angle between $[110]_o$ and $[\bar{1}10]_o$ crystallographic axes in the substrate. For simplicity, we assume that $\overline{\varepsilon'_{11}}=\overline{\varepsilon'_{22}}=0$ in our simulations. The energies of the eight polarization variants are no longer equal under the shear substrate strain. For a positive shear substrate strain, four of them ($r_1^{\pm}$ and $r_3^{\pm}$) have lower energy than the rest. However, as pointed out in Ref. 25, the twins formed by $r_1^{\pm}$ and $r_3^{\pm}$ are not expected to exist in $(001)_c$ oriented films, as they do not relax elastic energy but create additional domain wall energy. Similarly, the variants pairs r_1^+/r_1^- and r_3^+/r_3^- separated by 180° domain walls will not exist either. Therefore, with sufficient relaxation time, only one polarization variant will survive, and a single domain structure will be obtained [shown as Fig. 1(d)]. For a negative shear substrate strain, the other four variants ($r_2^{\pm}$ and $r_4^{\pm}$) have lower energy, and a single domain structure is again the stable state.

For a $(101)_c$ $BiFeO_3$ thin film deposited on a $(101)_c$ oriented cubic crystal substrate with an in-plane orientation relationship of $[010]_c^{BiFeO_3}\|[010]_c^s$, a constant dilatational strain is imposed in the x'_1-x'_2 plane,

$$\overline{\varepsilon'_{11}}=\overline{\varepsilon'_{22}}=\varepsilon_0, \quad \overline{\varepsilon'_{12}}=0, \tag{12}$$

where $\varepsilon_0=(a_s-a_{BiFeO_3})/a_{BiFeO_3}$. The spontaneous strains of the polarization variants in the coordinate system II can be calculated by Eq. (8), which give

$$(\varepsilon_{ij}^0)'_{r_1^{\pm}}=\begin{bmatrix}0 & 0 & 0.0076\\ 0 & -0.0054 & 0\\ 0 & 0 & 0.0054\end{bmatrix},$$

$$(\varepsilon_{ij}^0)'_{r_2^{\pm}}=\begin{bmatrix}0 & 0.0076 & 0\\ 0 & 0.0054 & 0\\ 0 & 0 & -0.0054\end{bmatrix},$$

$$(\varepsilon_{ij}^0)'_{r_3^{\pm}}=\begin{bmatrix}0 & -0.0076 & 0\\ 0 & 0.0054 & 0\\ 0 & 0 & -0.0054\end{bmatrix},$$

$$(\varepsilon_{ij}^0)'_{r_4^{\pm}}=\begin{bmatrix}0 & 0 & -0.0076\\ 0 & -0.0054 & 0\\ 0 & 0 & 0.0054\end{bmatrix}. \tag{13}$$

Figure 3 shows the domain structures of $(101)_c$ $BiFeO_3$ thin films under different substrate strains. For a large compressive substrate strain, it is clear that polarization variants $r_1^{\pm}$ and $r_4^{\pm}$ are favored energetically due to their negative

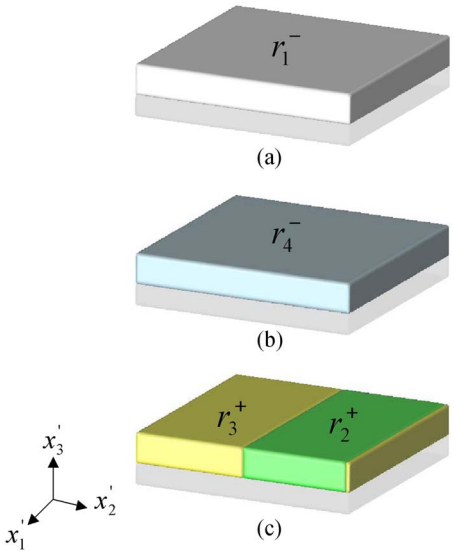

FIG. 3. (Color online) Domain structures of $(101)_c$ $BiFeO_3$ thin films. (a) $\overline{\varepsilon'_{11}}=\overline{\varepsilon'_{22}}=-0.005, \overline{\varepsilon'_{12}}=0$; (b) $\overline{\varepsilon'_{11}}=\overline{\varepsilon'_{22}}=0, \overline{\varepsilon'_{12}}=0$; and (c) $\overline{\varepsilon'_{11}}=\overline{\varepsilon'_{22}}=0.005, \overline{\varepsilon'_{12}}=0$.

normal spontaneous strains in $(101)_c$ plane (x'_1-x'_2 plane). However, the polarization variants r_1 and r_4 have the same spontaneous deformation in the $(101)_c$ plane, therefore, the twin structure formed by these variants will not relax elastic energy and is not expected to exist. As shown in Fig. 3(a), the equilibrium domain structure is a single domain. On the other hand, for a large tensile substrate strain, the polarization variants $r_2^{\pm}$ and $r_3^{\pm}$ are energetically favored. In this case, a twin structure is more stable [shown as Fig. 3(c)], as the spontaneous strains of r_2 and r_3 have opposite shear components in the $(101)_c$ plane. When the substrate strains are close to zero, quite different domain structures were obtained from phase-field simulations, depending on the initial random values used, since the energy difference between various domain structures is quite small in this case. Figure 3(b) shows one example of the domain structures obtained for $\varepsilon_0=0$. We also calculated the volume average of the spontaneous polarization over the domain structure for the three different substrate constraints: (a) $\overline{P_s}=0.922$, (b) $\overline{P_s}=0.910$, and (c) $\overline{P_s}=0.910$ (unit: C m^{-2}). We can see that the effect of the normal substrate strain on the spontaneous polarization is relatively large comparing with the $(001)_c$ films, which is consistent with our previous thermodynamic calculations.[23]

For a $(111)_c$ oriented $BiFeO_3$ thin film deposited on a $(111)_c$ oriented cubic crystal substrate with an in-plane orientation relationship of $[1\bar{1}0]_c^{BiFeO_3}\|[1\bar{1}0]_c^s$, a constant dilatational strain is imposed in the x'_1-x'_2 plane,

$$\overline{\varepsilon'_{11}}=\overline{\varepsilon'_{22}}=\varepsilon_0, \quad \overline{\varepsilon'_{12}}=0 \tag{14}$$

where $\varepsilon_0=(a_s-a_{BiFeO_3})/a_{BiFeO_3}$. The spontaneous strains of the polarization variants in the coordinate system II are given by

$$(\varepsilon_{ij}^0)'_{r_1^{\pm}}=\begin{bmatrix}-0.0054 & 0 & 0\\ 0 & -0.0054 & 0\\ 0 & 0 & 0.0108\end{bmatrix},$$

Downloaded 19 Oct 2008 to 66.71.79.131. Redistribution subject to AIP license or copyright; see http://jap.aip.org/jap/copyright.jsp

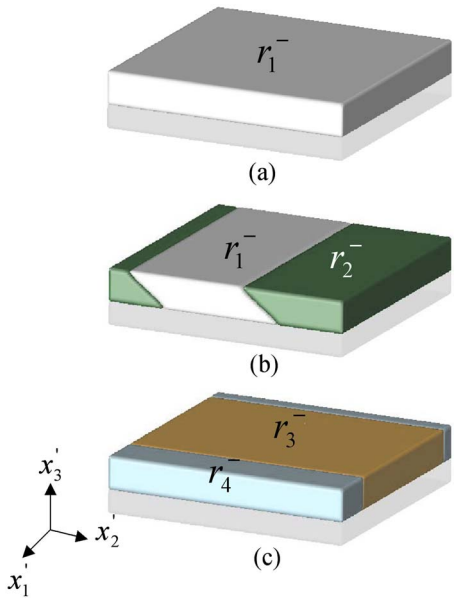

FIG. 4. (Color online) Domain structures of $(111)_c$ $BiFeO_3$ thin films. (a) $\overline{\varepsilon'_{11}}=\overline{\varepsilon'_{22}}=-0.005, \overline{\varepsilon'_{12}}=0$; (b) $\overline{\varepsilon'_{11}}=\overline{\varepsilon'_{22}}=0, \overline{\varepsilon'_{12}}=0$; and (c) $\overline{\varepsilon'_{11}}=\overline{\varepsilon'_{22}}=0.005, \overline{\varepsilon'_{12}}=0$.

$$(\varepsilon_{ij}^0)'_{r_2^\pm}=\begin{bmatrix}-0.0054 & 0 & 0\\ 0 & 0.0090 & 0.0051\\ 0 & 0 & -0.0036\end{bmatrix},$$

$$(\varepsilon_{ij}^0)'_{r_3^\pm}=\begin{bmatrix}0.0054 & -0.0062 & 0.0044\\ 0 & -0.0018 & -0.0025\\ 0 & 0 & -0.0036\end{bmatrix},$$

$$(\varepsilon_{ij}^0)'_{r_4^\pm}=\begin{bmatrix}0.0054 & 0.0062 & -0.0044\\ 0 & -0.0018 & -0.0025\\ 0 & 0 & -0.0036\end{bmatrix}. \quad (15)$$

Figure 4 shows the stable domain structures of $(111)_c$ $BiFeO_3$ thin films under different substrate strains. For a large compressive substrate strain, the polarization variants perpendicular to the film surface ($r_1^\pm$) have the lowest energy. The stable domain structure is a single domain with either up or down polarization, since existence of both variants will create additional domain wall energy. While for a large tensile substrate strain, the other six polarization variants ($r_2^\pm$, $r_3^\pm$, and $r_4^\pm$) are more favored energetically, and the domain structure obtained is a twin structure [shown as Fig. 4(c)] that relaxes the elastic energy. When the substrate strains are close to zero, the energy differences between various domain structures are relatively small, and domain structures different from Fig. 4(b) were obtained from our simulations with exactly same parameters but different initial random polarization distributions. We also calculated the volume average of the spontaneous polarization over the domain structure for the three different substrate constraints: (a) $\overline{P_s}=0.915$, (b) $\overline{P_s}=0.906$, and (c) $\overline{P_s}=0.908$ (unit: C m^{-2}). We can see that the spontaneous polarization of the $BiFeO_3$ thin films is increased by the normal compressive substrate strains, and the normal tensile substrate strains to a lesser extent, which is in agreement with the thermodynamic calculations.[23]

IV. SUMMARIES AND CONCLUSIONS

Phase-field simulations were conducted in the present work to study the ferroelectric domain structures in $(001)_c$, $(101)_c$, and $(111)_c$ oriented epitaxial $BiFeO_3$ thin films. It was found that the domain structures of $(001)_c$ $BiFeO_3$ thin film are not sensitive to the normal substrate strains, and twinlike domain structures were observed for the full range of substrate strains. The orientations of $\{110\}_c$-type domain walls are determined by the competition between total domain wall energy and elastic energy. While a single domain structure was obtained for $(001)_c$ oriented film under a shear substrate strain. On the other hand, for $(101)_c$ and $(111)_c$ oriented $BiFeO_3$ thin films, it was demonstrated that the normal substrate strains can effectively alter the domain structures. It should be noted that, in addition to the substrate strains studied in this work, there are several other factors that could also be important for the domain structures of ferroelectric thin films, for example, the electric boundary conditions[26] and film thickness.[27]

ACKNOWLEDGMENTS

The authors are grateful for the financial support by the National Science Foundation under the Grant Nos. DMR-0507146 and DMR-0213623, by the Department of Energy under the Grant No. DE-FG02-07ER46417, the Penn State MRI seed grant, and the Laboratory-Directed Research and Development at Los Alamos National Laboratory.

[1] J. Wang, J. B. Neaton, H. Zheng, V. Nagarajan, S. B. Ogale, B. Liu, D. Viehland, V. Vaithyanathan, D. G. Schlom, U. V. Waghmare, N. A. Spaldin, K. M. Rabe, M. Wuttig, and R. Ramesh, Science **299**, 1719 (2003).
[2] Y. P. Wang, L. Zhou, M. F. Zhang, X. Y. Chen, J. M. Liu, and Z. G. Liu, Appl. Phys. Lett. **84**, 1731 (2004).
[3] J. F. Li, J. Wang, M. Wuttig, R. Ramesh, N. G. Wang, B. Ruette, A. P. Pyatakov, A. K. Zvezdin, and D. Viehland, Appl. Phys. Lett. **84**, 5261 (2004).
[4] J. Wang, H. Zheng, Z. Ma, S. Prasertchoung, M. Wuttig, R. Droopad, J. Yu, K. Eisenbeiser, and R. Ramesh, Appl. Phys. Lett. **85**, 2574 (2004).
[5] K. Y. Yun, M. Noda, M. Okuyama, H. Saeki, H. Tabata, and K. Saito, J. Appl. Phys. **96**, 3399 (2004).
[6] C. Ederer and N. A. Spaldin, Phys. Rev. B **71**, 224103 (2005).
[7] T. Zhao, A. Scholl, F. Zavaliche, K. Lee, M. Barry, A. Doran, M. P. Cruz, Y. H. Chu, C. Ederer, N. A. Spaldin, R. R. Das, D. M. Kim, S. H. Baek, C. B. Eom, and R. Ramesh, Nat. Mater. **5**, 823 (2006).
[8] R. Ramesh and N. A. Spaldin, Nat. Mater. **6**, 21 (2007).
[9] F. Zavaliche, R. R. Das, D. M. Kim, C. B. Eom, S. Y. Yang, P. Shafer, and R. Ramesh, Appl. Phys. Lett. **87**, 182912 (2005).
[10] F. Zavaliche, P. Shafer, R. Ramesh, M. P. Cruz, R. R. Das, D. M. Kim, and C. B. Eom, Appl. Phys. Lett. **87**, 252902 (2005).
[11] R. R. Das, D. M. Kim, S. H. Baek, C. B. Eom, F. Zavaliche, S. Y. Yang, R. Ramesh, Y. B. Chen, X. Q. Pan, X. Ke, M. S. Rzchowski, and S. K. Streiffer, Appl. Phys. Lett. **88**, 242904 (2006).
[12] Y. B. Chen, M. B. Katz, X. Q. Pan, R. R. Das, D. M. Kim, S. H. Baek, and C. B. Eom, Appl. Phys. Lett. **90**, 072907 (2007).
[13] Y. H. Chu, Q. Zhan, L. W. Martin, M. P. Cruz, P. Yang, F. Zavaliche, S. Y. Yang, J. X. Zhang, L. Q. Chen, D. G. Schlom, I. N. Lin, T. B. Wu, and R. Ramesh, Adv. Mater. (Weinheim, Ger.) **18**, 2307 (2006).
[14] Y. H. Chu, M. P. Cruz, C. H. Yang, L. W. Martin, P. L. Yang, J. X. Zhang, K. Lee, P. Yu, L. Q. Chen, and R. Ramesh, Adv. Mater. (Weinheim, Ger.) **19**, 2662 (2007).
[15] H. L. Hu and L. Q. Chen, Mater. Sci. Eng., A **238**, 182 (1997).
[16] Y. L. Li, S. Y. Hu, Z. K. Liu, and L. Q. Chen, Appl. Phys. Lett. **78**, 3878

Downloaded 19 Oct 2008 to 66.71.79.131. Redistribution subject to AIP license or copyright; see http://jap.aip.org/jap/copyright.jsp

(2001).
[17]Y. L. Li, S. Y. Hu, Z. K. Liu, and L. Q. Chen, Acta Mater. **50**, 395 (2002).
[18]Y. L. Li, L. Q. Chen, G. Asayama, D. G. Schlom, M. A. Zurbuchen, and S. K. Streiffer, J. Appl. Phys. **95**, 6332 (2004).
[19]S. Choudhury, Y. L. Li, C. E. Krill III, and L. Q. Chen, Acta Mater. **53**, 5313 (2005).
[20]A. G. Khachaturyan, *Theory of Structural Transformation in Solids* (Wiley, New York, 1983), p. 198.
[21]A. N. Stroh, J. Math. Phys. **41**, 77 (1962).
[22]L. Q. Chen and J. Shen, Comput. Phys. Commun. **108**, 147 (1998).
[23]J. X. Zhang, Y. L. Li, Y. Wang, Z. K. Liu, L. Q. Chen, Y. H. Chu, F. Zavaliche, and R. Ramesh, and J. Appl. Phys. **101**, 114105 (2007).
[24]The fourth-order coefficients (a_{11} and a_{12}) are for the stress-free boundary condition, which are related to those for the clamped boundary condition (Ref. 23) by

$$a_{11} = a_{11}^{\text{clamped}} - \left[\tfrac{1}{2}C_{1111}(Q_{1111}^2 + 2Q_{1122}^2) + C_{1122}Q_{1122}(2Q_{1111} + Q_{1122})\right],$$

$$a_{12} = a_{12}^{\text{clamped}} - [C_{1111}Q_{1122}(2Q_{1111} + Q_{1122}) + C_{1122}(Q_{1111}^2 + 3Q_{1122}^2 + 2Q_{1111}Q_{1122}) + 8C_{1212}Q_{1212}^2].$$

[25]S. K. Streiffer, C. B. Parker, A. E. Romanov, M. J. Lefevre, L. Zhao, J. S. Speck, W. Pompe, C. M. Foster, and G. R. Bai, J. Appl. Phys. **83**, 2742 (1998).
[26]Y. L. Li, S. Y. Hu, and L. Q. Chen, J. Appl. Phys. **97**, 034112 (2005).
[27]Y. H. Chu, T. Zhao, M. P. Cruz, Q. Zhan, P. L. Yang, L. W. Martin, M. Huijben, C. H. Yang, F. Zavaliche, H. Zheng, and R. Ramesh, Appl. Phys. Lett. **90**, 252906 (2007).

Downloaded 19 Oct 2008 to 66.71.79.131. Redistribution subject to AIP license or copyright; see http://jap.aip.org/jap/copyright.jsp